Properties of cosmic Deuterons and ^{3}He

F. Dimiccoli & P. Zuccon (Trento University and INFN)

Why Z=1&2 isotopes?

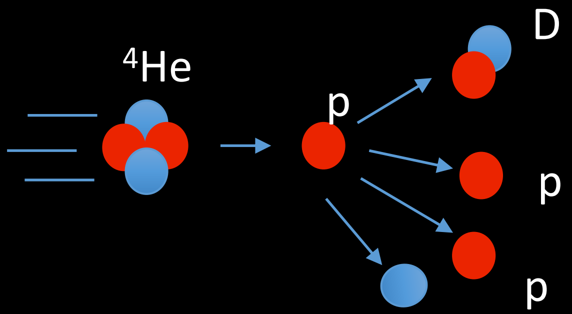

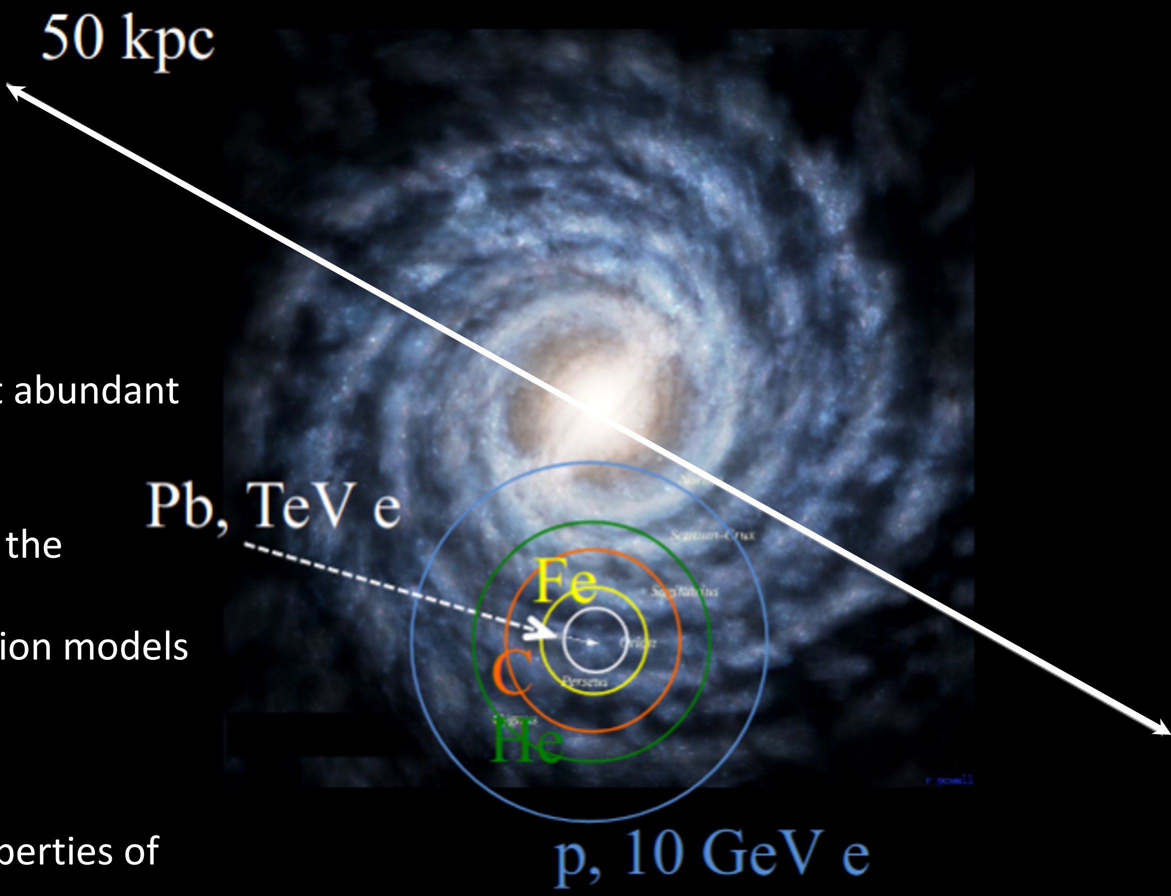

- Helium nuclei are the second most abundant nuclei in cosmic rays.
- D and ^{3}He are mostly produced by the fragmentation of ^{4}He: simpler comparison with propagation models wrt heavy nuclei
- Smaller cross section of He: D/^{4}He and ^{3}He/^{4}He probe the properties of diffusion at larger distances
- Different A/Z ratios of D and ^{3}He allow to disentangle kinetic energy and rigidity dependence of propagation.

Light isotope measurements with AMS02

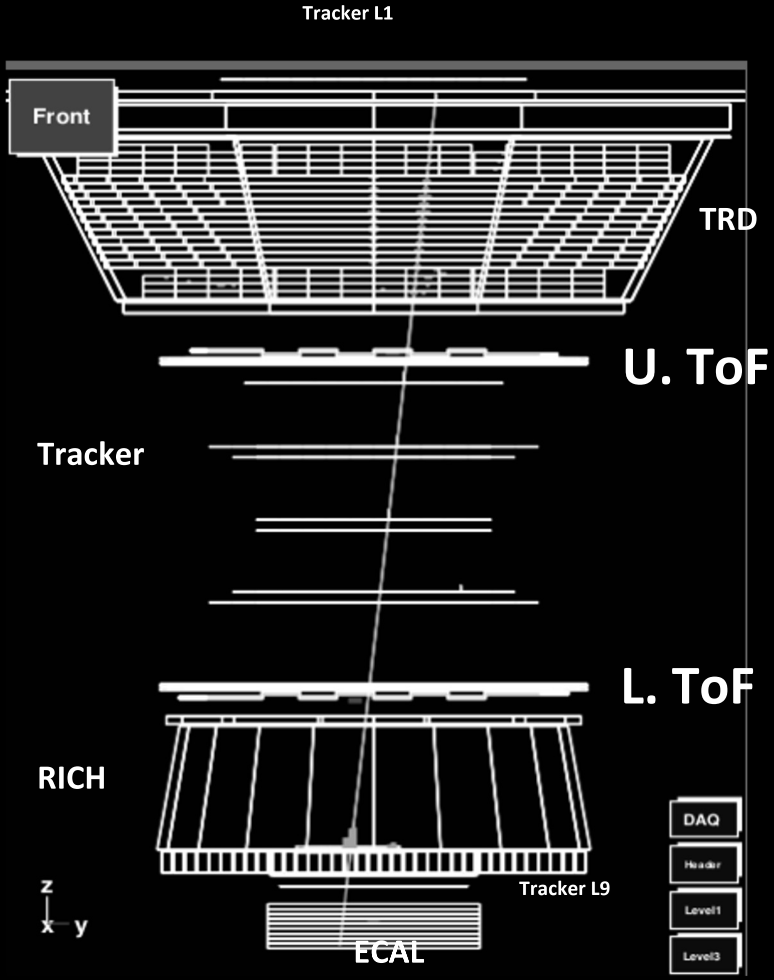

- AMS is composed by different sub-detectors for the redundant ID of the elements in CR
- The **Mass** is identified from the concurrent measurement of **Rigidity, Velocity** and **Charge**
- **Mass resolution** not good enough for event-by-event isotope ID -> Fit of distribution

TOF	$\sigma_\beta/\beta \sim 3\%$	$0.2 < E_k < 1.1$ GeV/n
RICH NaF	$\sigma_\beta/\beta \sim 0.3\%$	$0.7 < E_k < 3.7$ GeV/n
RICH AgI	$\sigma_\beta/\beta \sim 0.1\%$	$2.6 < E_k < 8.9$ GeV/n

Isotope separation:

rigidity

abs. charge

$$m = \frac{RZ}{\beta\gamma}$$

mass

speed / c

$$\left(\frac{\Delta m}{m}\right)^2 \cong \left(\frac{\Delta R}{R}\right)^2 + \gamma^4\left(\frac{\Delta\beta}{\beta}\right)^2$$

~ 10 %

~3 %
~0.3 %
~ 0.1 %

Z=1

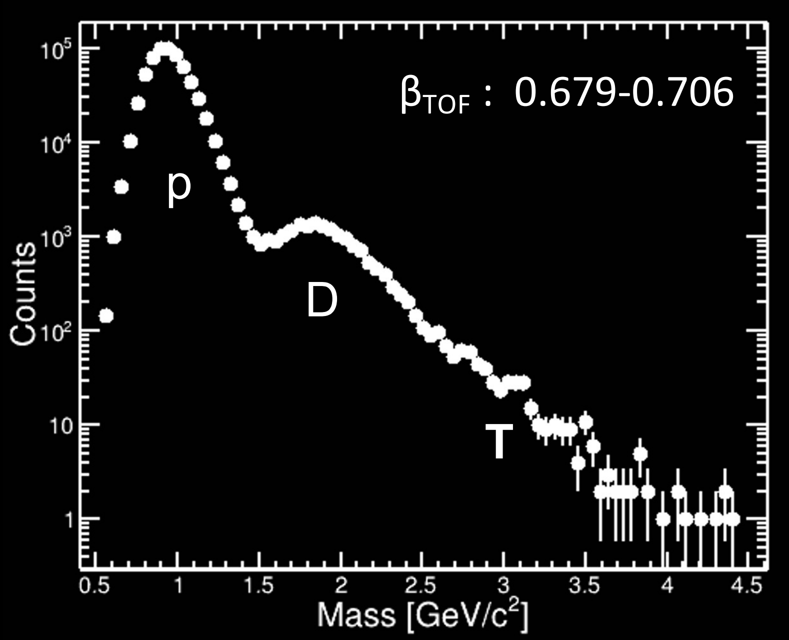

Z=2

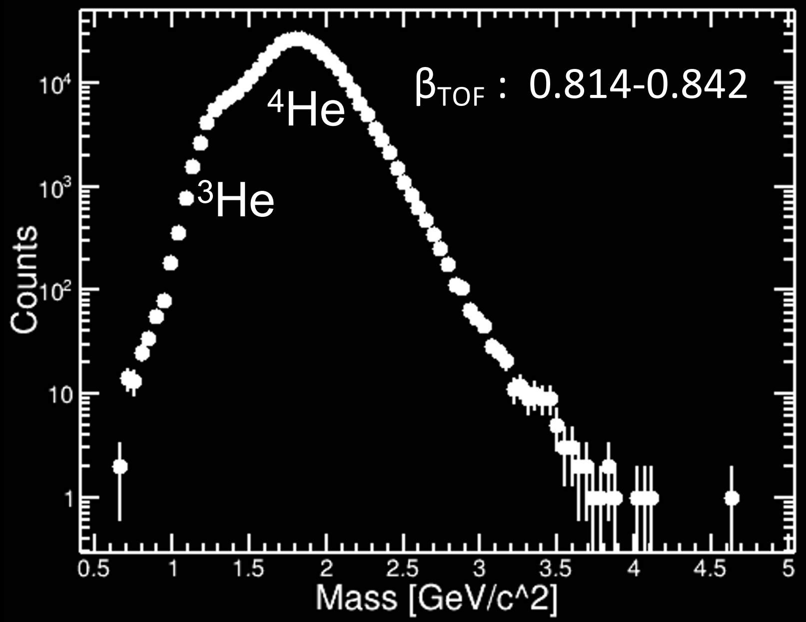

Method1: Isotope template fitting

The separation power depends on rigidity and velocity (β) resolutions

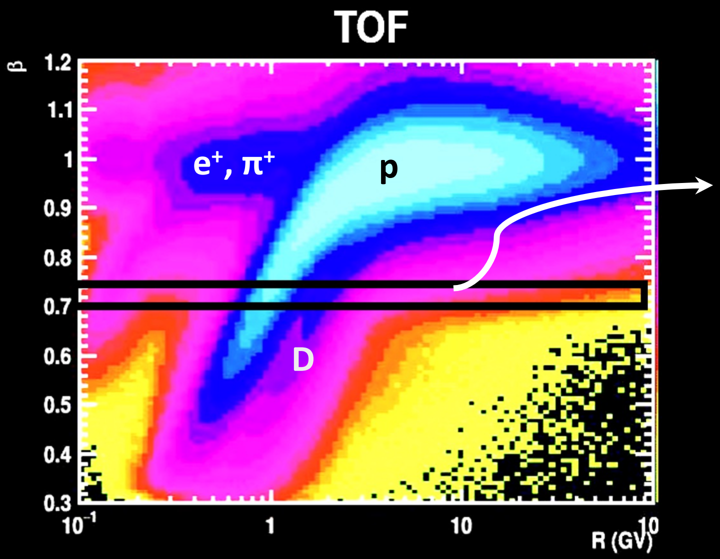

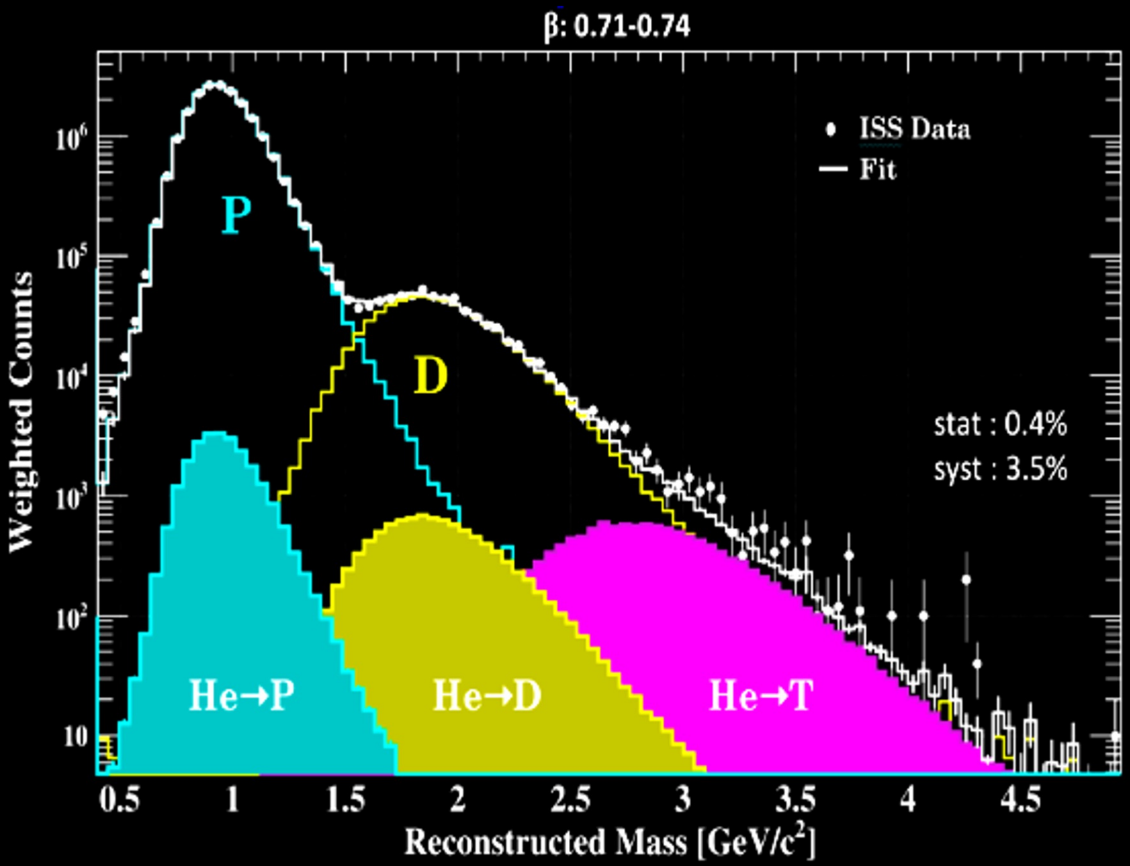

Fit of the mass with templates from MC

- MC templates tuned using data
- data driven estim. fragmentation from Z>1
- D'Agostini iterative method for bin-to-bin migration

Fit to data (on Mass distributions)

The two remaining free parameters (σ_1 and μ_1) are fixed bin-by-bin directly fitting the mass distributions

- NxN mass templates obtained changing σ_1 and μ_1 in a ±20% range
- Independent fit for every template
- **Marginalization:** To every template a weight is assigned: $w = \exp(-\chi^2 / 2)$

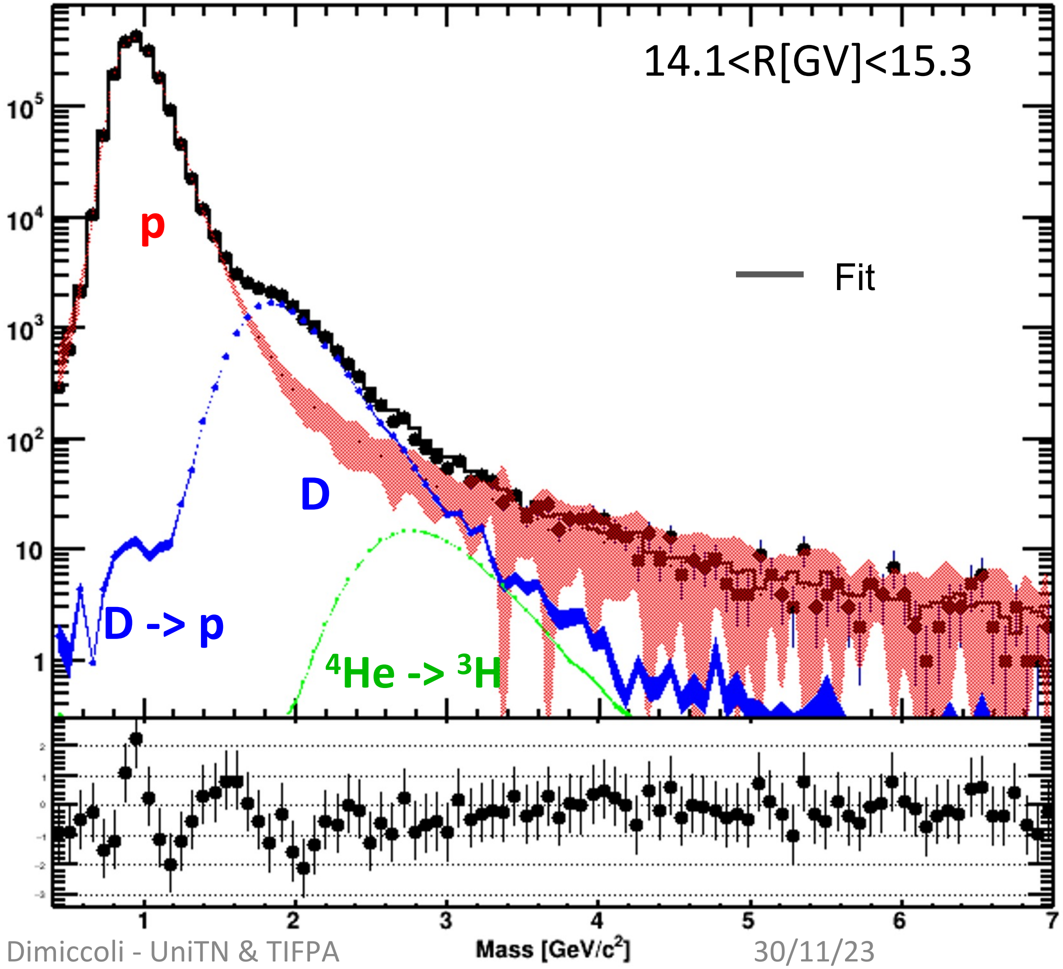

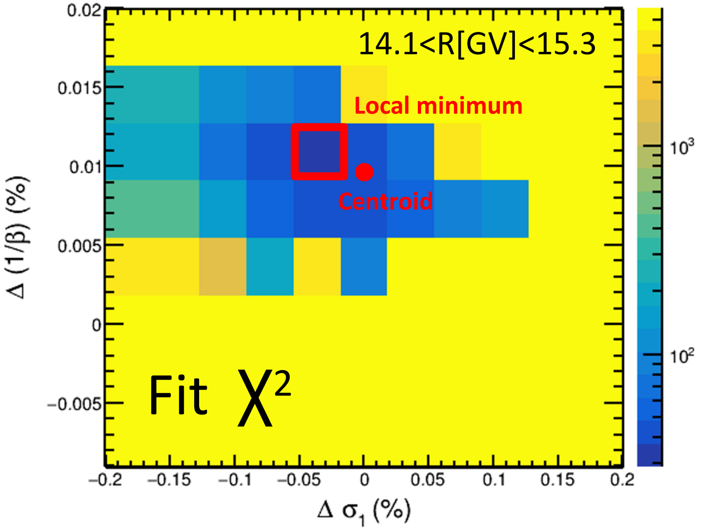

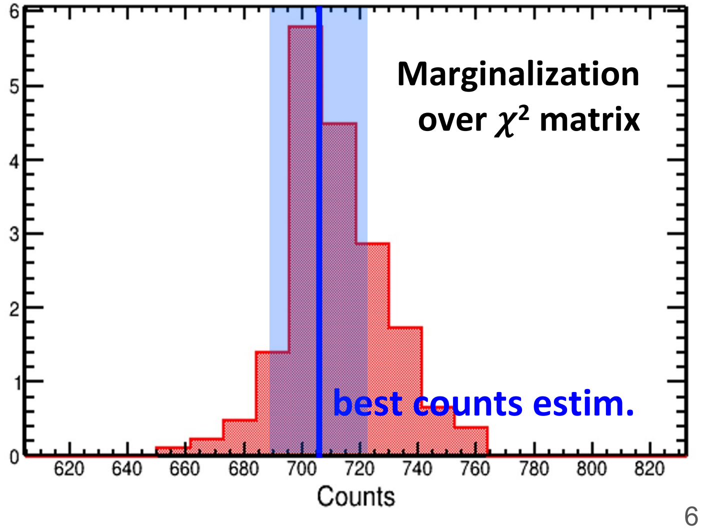

Z=1 and Z=2 Template fits

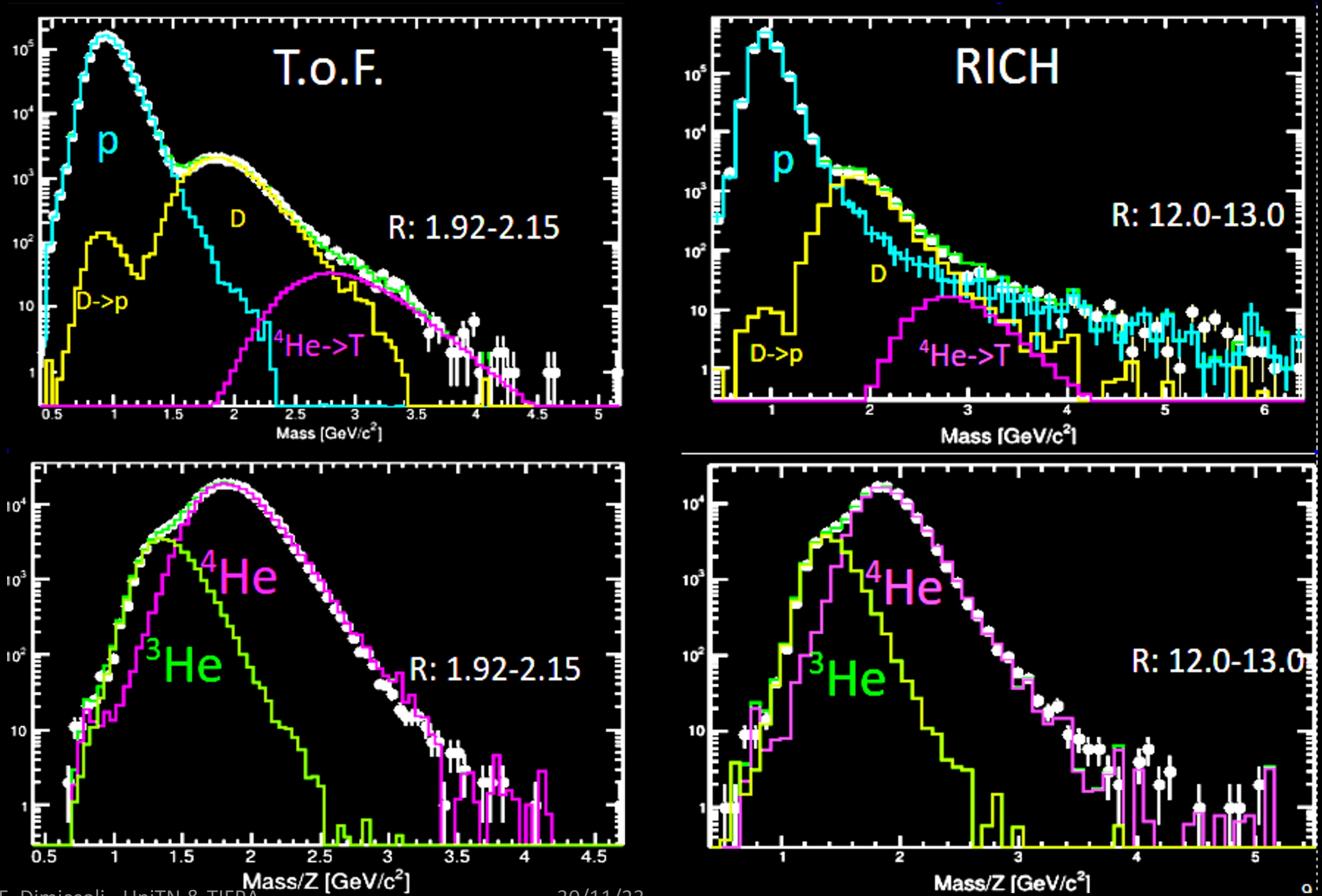

Trends for the free parameter were extracted as a function of:

Energy

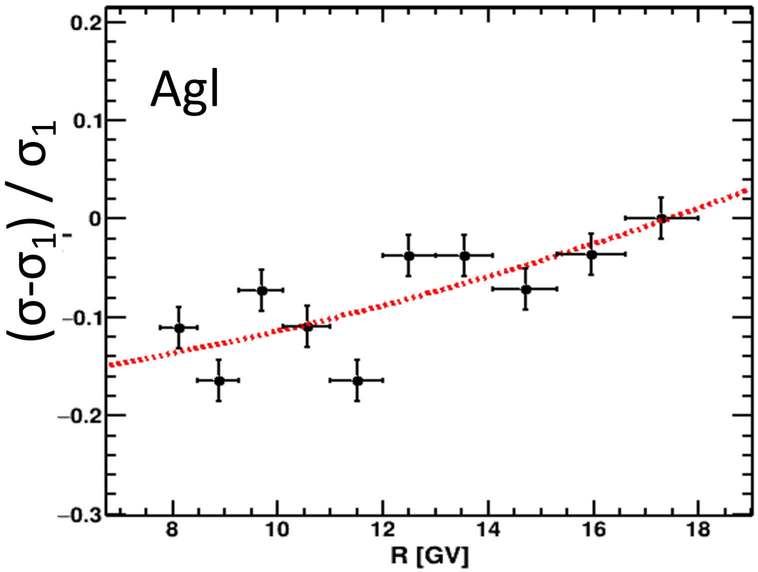

Time

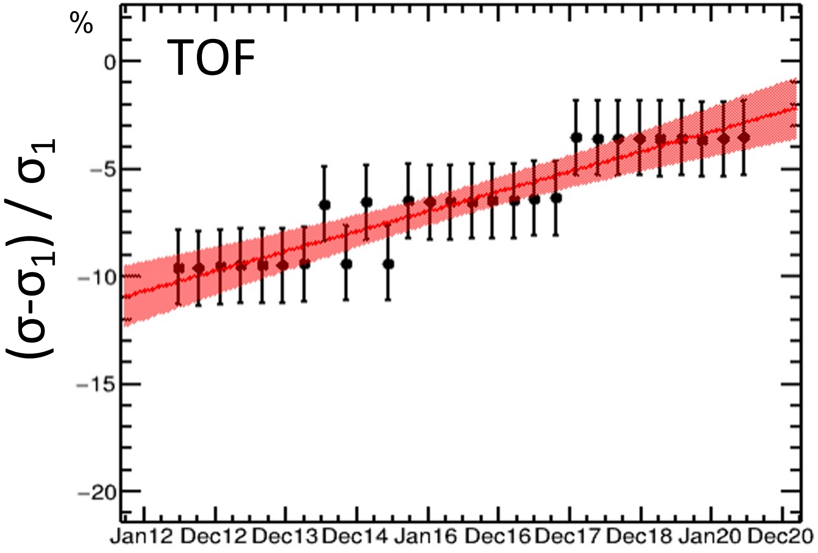

The stability of fit results were also checked to be stable against time

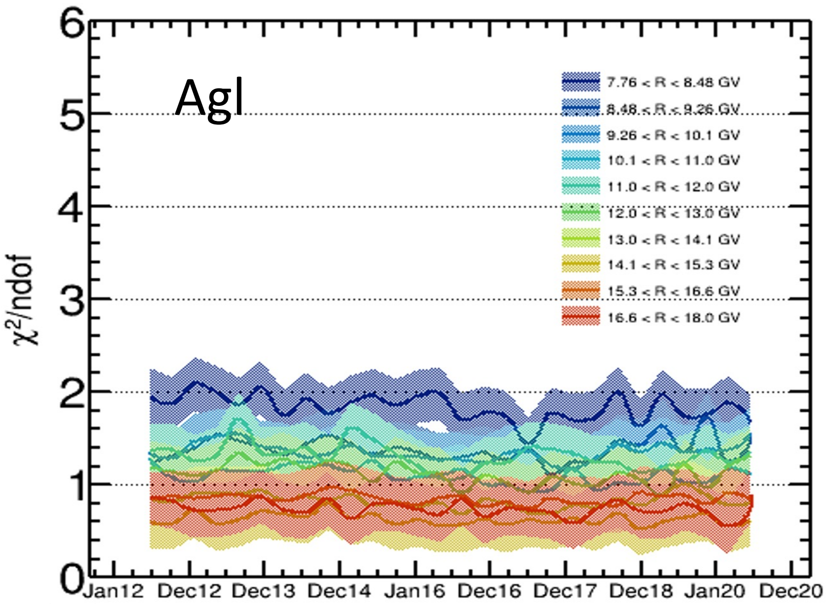

Method2: Global bi-dimensional unfolding on R vs β distributions

- Migration matrices for R and β from MC (iteratively adapted to data)
- Fit on the total Z=1(2) data distribution for TOF, NaF and Agl (assumption: unique continuous flux)

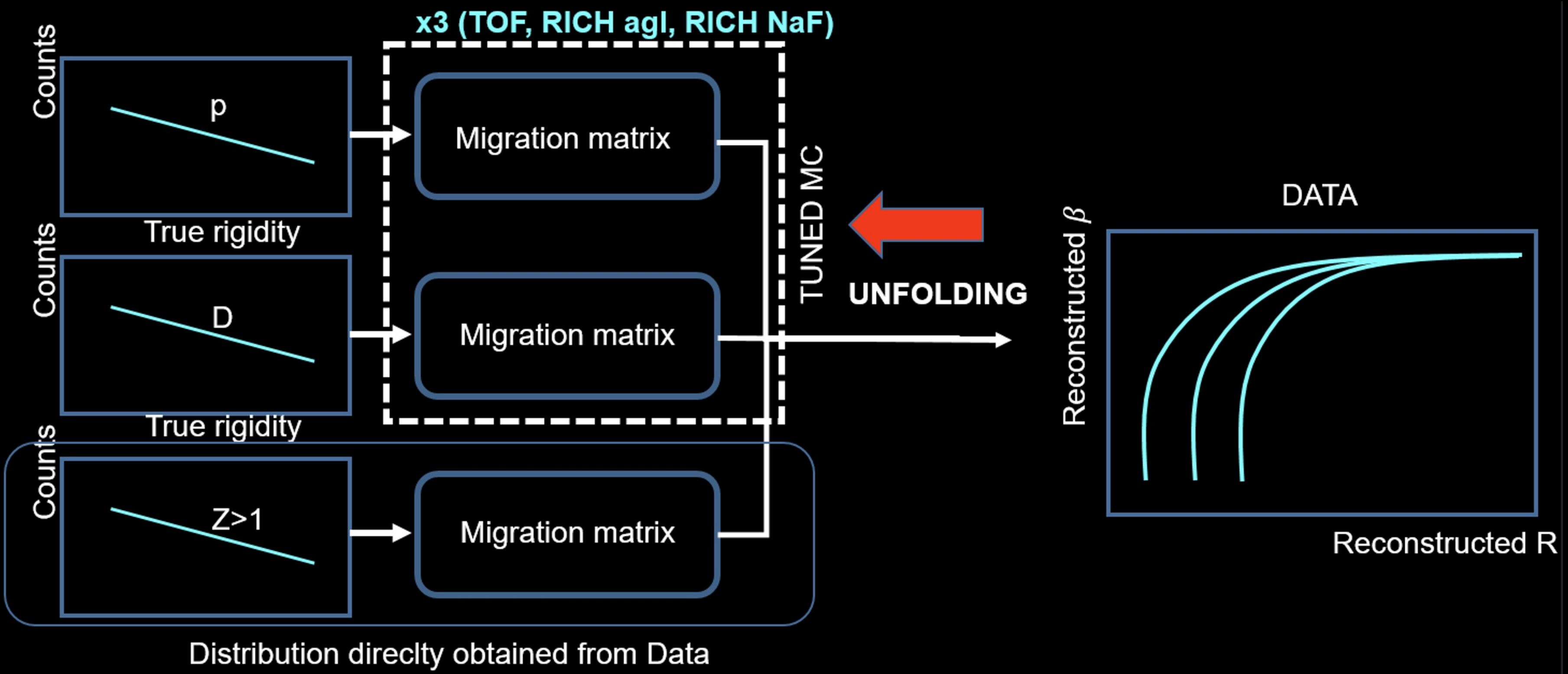

Deuteron Fluxes

MC templates carry informations about:

- Detector Efficiency
- Bin-to-bin migration

It is possible to directly use them to calculate **Acceptance** and **Unfolding factor** to normalize the counts and obtain **fluxes**

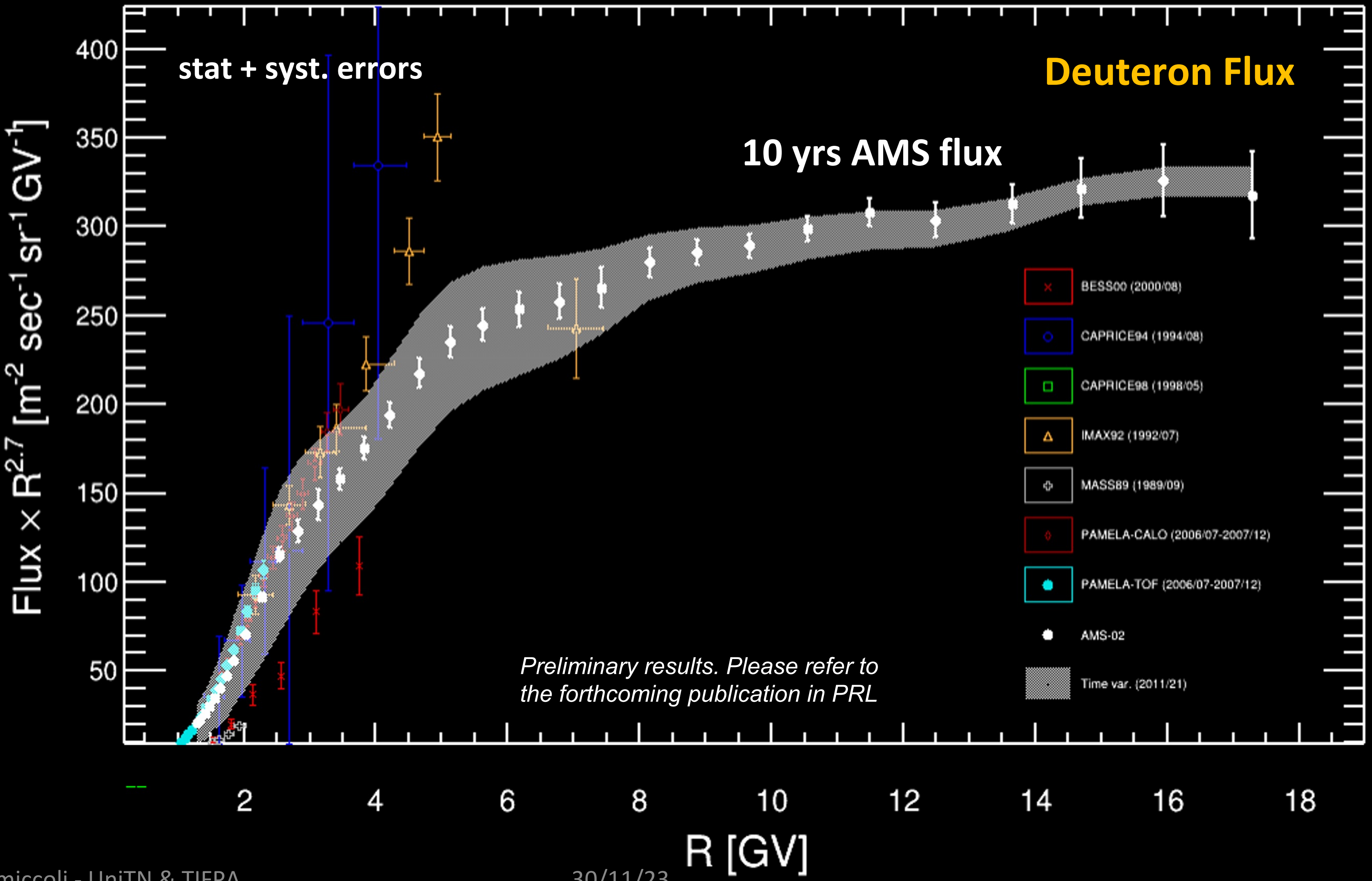

Preliminary results. Please refer to the forthcoming publication in PRL

Helium-3 Flux

MC templates carry informations about:

- Detector Efficiency
- Bin-to-bin migration

It is possible to directly use them to calculate **Acceptance** and **Unfolding factor** to normalize the counts and obtain **fluxes**

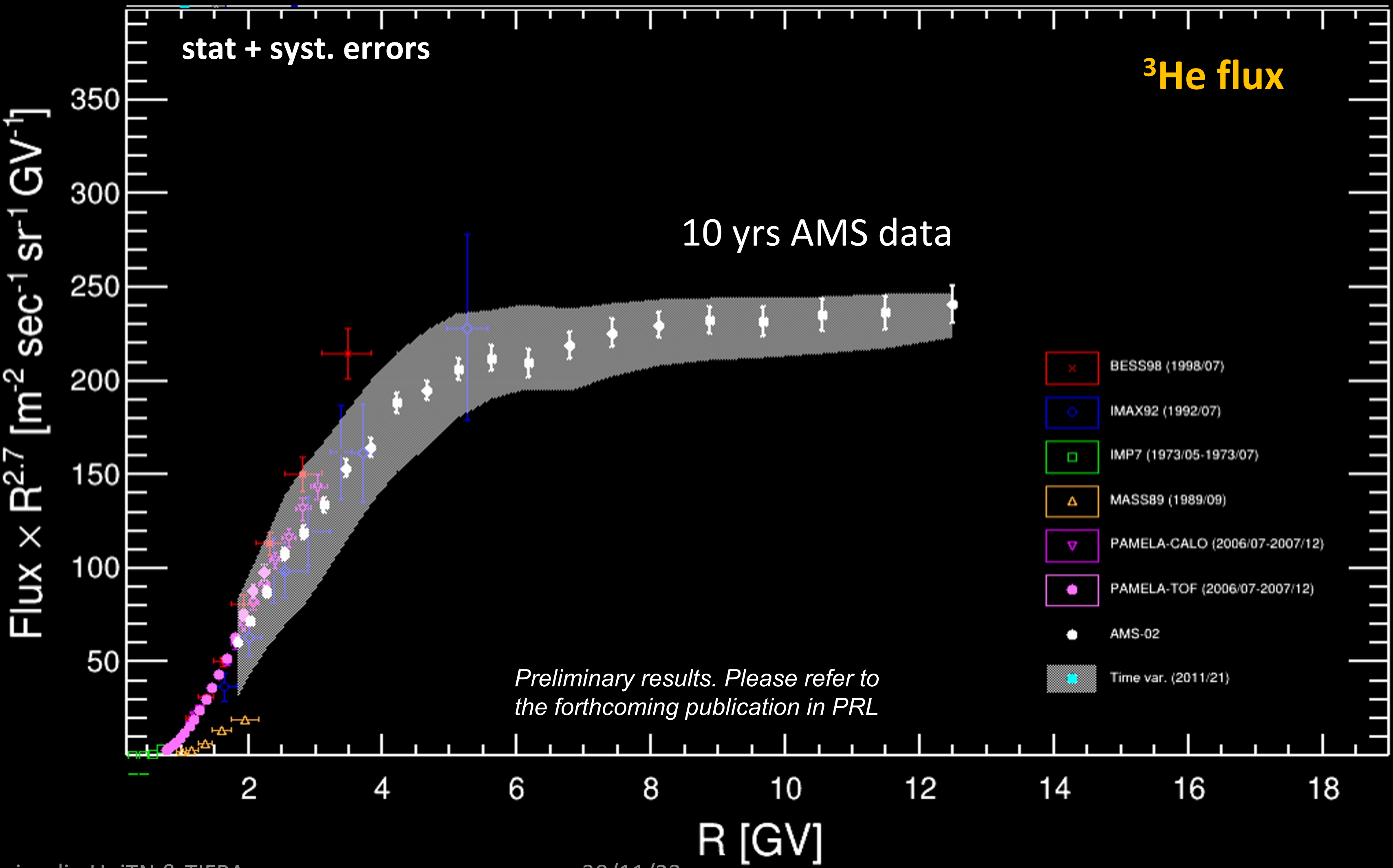

Preliminary results. Please refer to the forthcoming publication in PRL

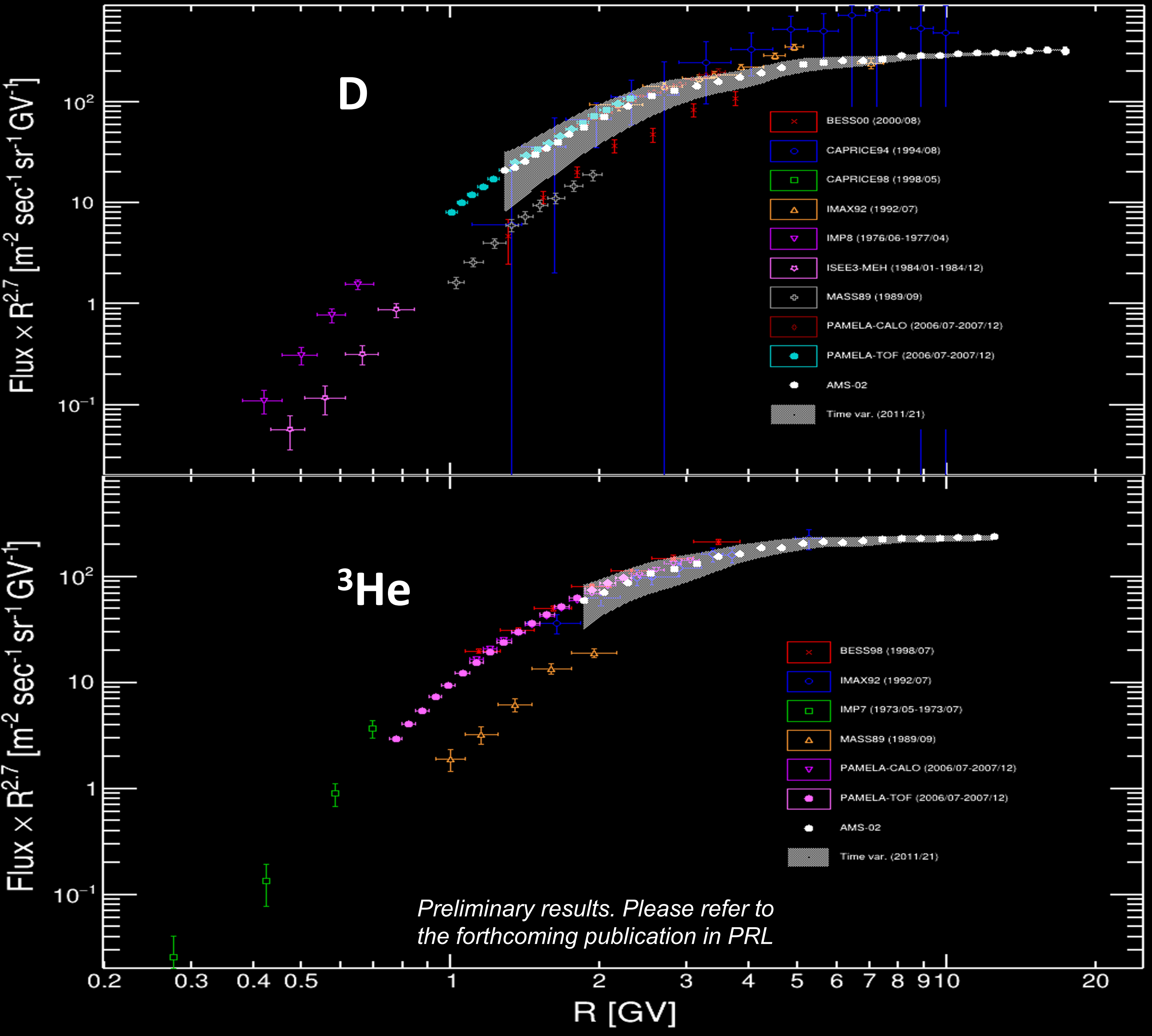

Preliminary results. Please refer to the forthcoming publication in PRL

Fluxes time dependence

- Time variation are visible above systematics only below ~ 5 GV
- ^{2}H and ^{3}He qualitatively follow the same time evolution of ^{4}He
- More sophisticated analysis is needed

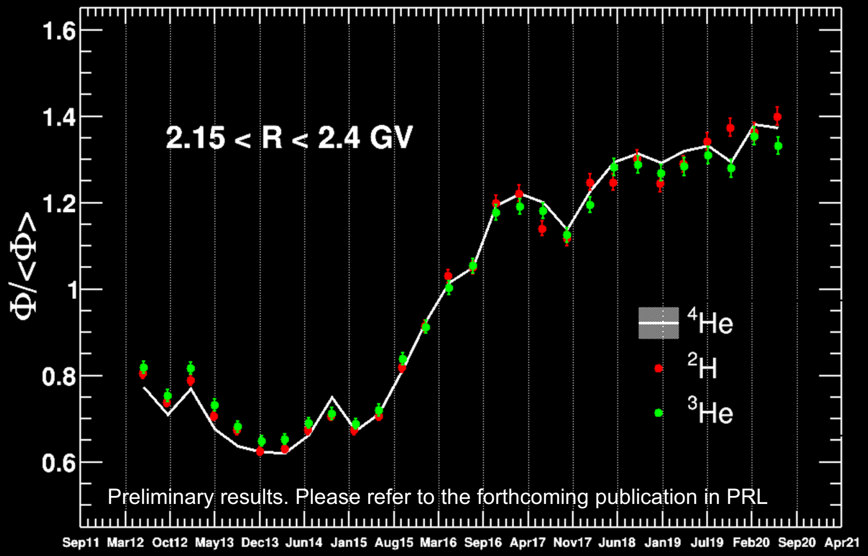

Preliminary results. Please refer to the forthcoming publication in PRL

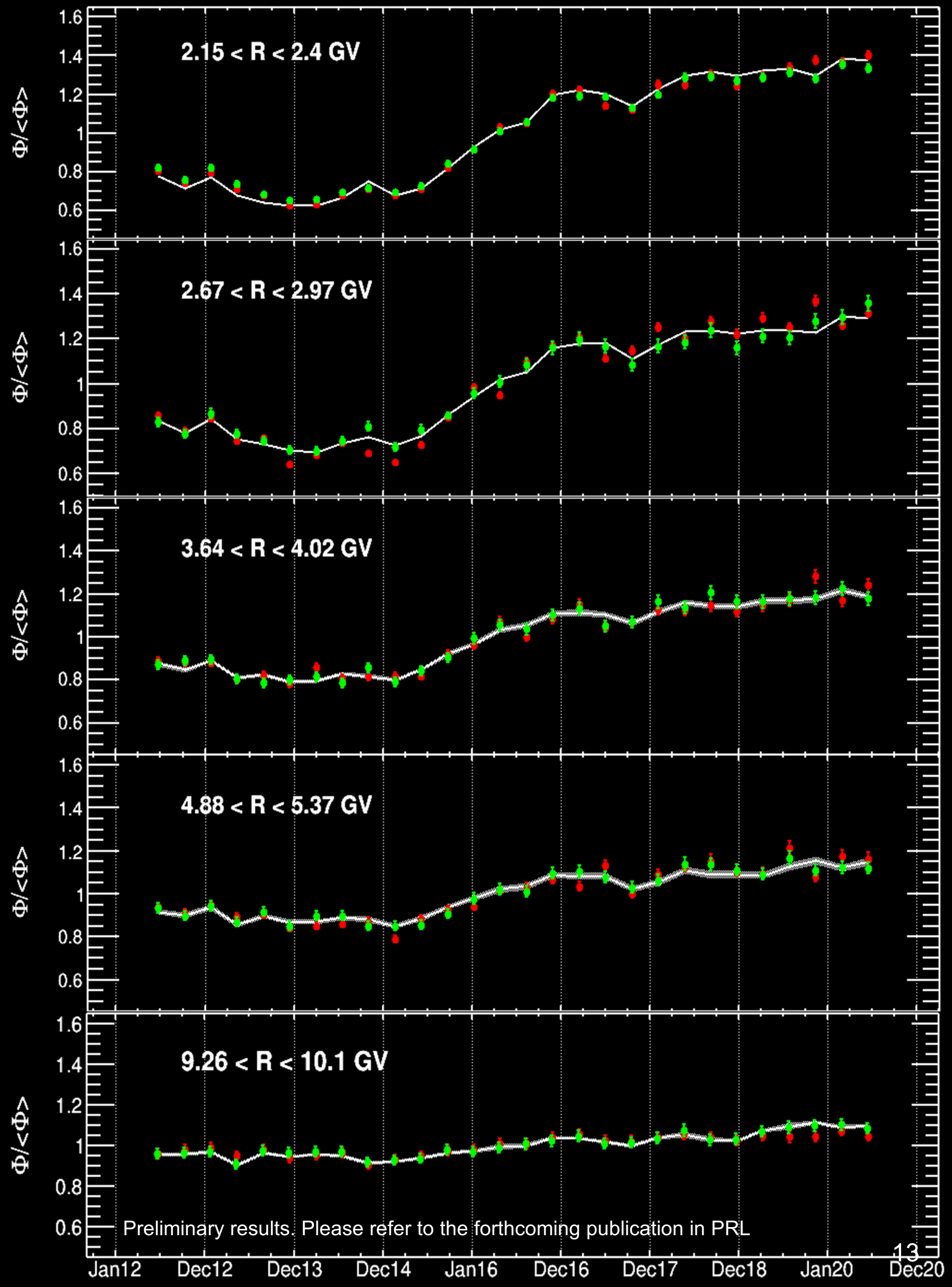

Preliminary results. Please refer to the forthcoming publication in PRL

Draft of D and ^{3}He paper

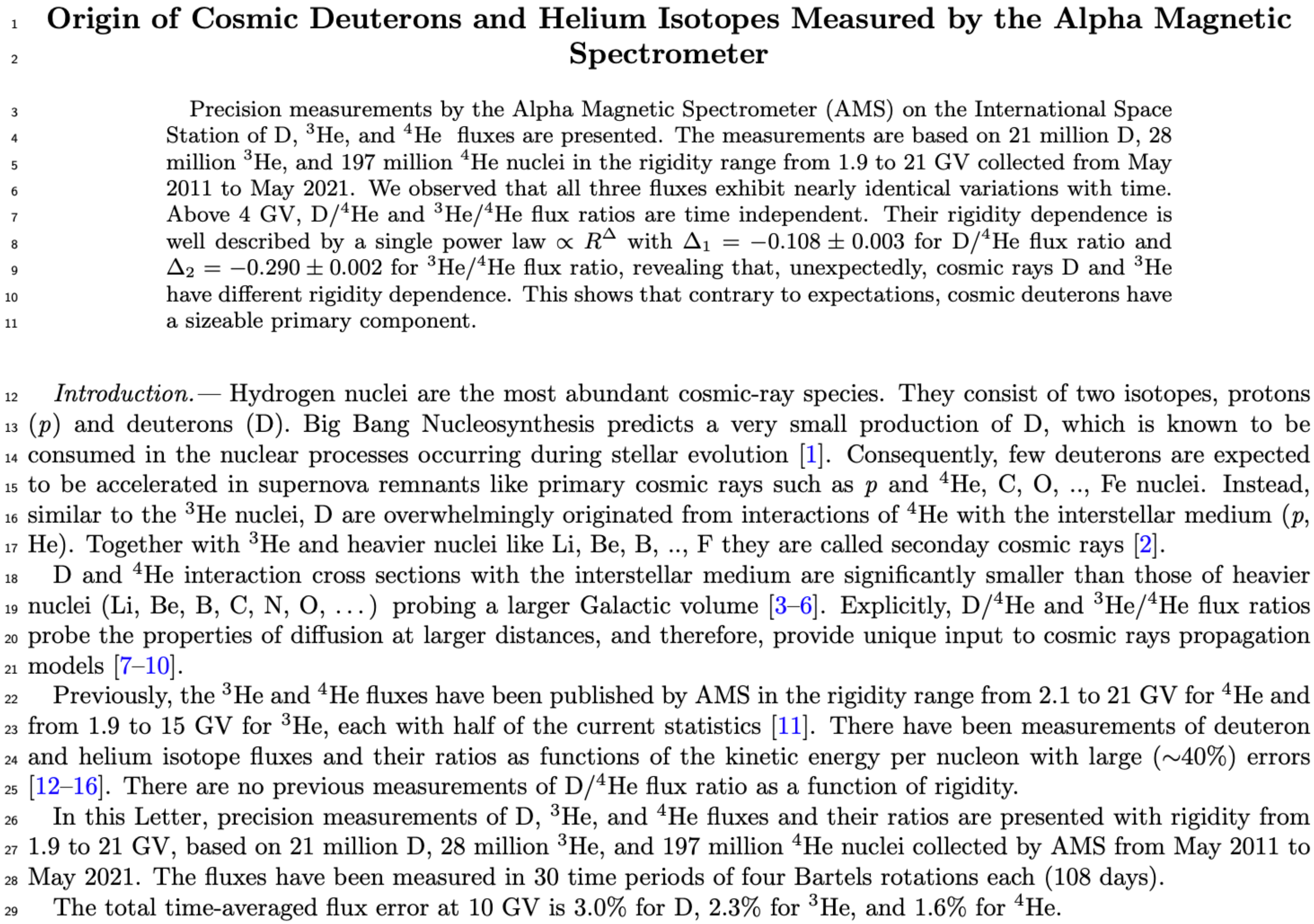

Origin of Cosmic Deuterons and Helium Isotopes Measured by the Alpha Magnetic Spectrometer

Precision measurements by the Alpha Magnetic Spectrometer (AMS) on the International Space Station of D, ^{3}He, and ^{4}He fluxes are presented. The measurements are based on 21 million D, 28 million ^{3}He, and 197 million ^{4}He nuclei in the rigidity range from 1.9 to 21 GV collected from May 2011 to May 2021. We observed that all three fluxes exhibit nearly identical variations with time. Above 4 GV, D/^{4}He and ^{3}He/^{4}He flux ratios are time independent. Their rigidity dependence is well described by a single power law $\propto R^{\Delta}$ with $\Delta_1 = -0.108 \pm 0.003$ for D/^{4}He flux ratio and $\Delta_2 = -0.290 \pm 0.002$ for ^{3}He/^{4}He flux ratio, revealing that, unexpectedly, cosmic rays D and ^{3}He have different rigidity dependence. This shows that contrary to expectations, cosmic deuterons have a sizeable primary component.

Introduction.— Hydrogen nuclei are the most abundant cosmic-ray species. They consist of two isotopes, protons (p) and deuterons (D). Big Bang Nucleosynthesis predicts a very small production of D, which is known to be consumed in the nuclear processes occurring during stellar evolution [1]. Consequently, few deuterons are expected to be accelerated in supernova remnants like primary cosmic rays such as p and ^{4}He, C, O, .., Fe nuclei. Instead, similar to the ^{3}He nuclei, D are overwhelmingly originated from interactions of ^{4}He with the interstellar medium (p, He). Together with ^{3}He and heavier nuclei like Li, Be, B, .., F they are called seconday cosmic rays [2].

D and ^{4}He interaction cross sections with the interstellar medium are significantly smaller than those of heavier nuclei (Li, Be, B, C, N, O, . . .) probing a larger Galactic volume [3–6]. Explicitly, D/^{4}He and ^{3}He/^{4}He flux ratios probe the properties of diffusion at larger distances, and therefore, provide unique input to cosmic rays propagation models [7–10].

Previously, the ^{3}He and ^{4}He fluxes have been published by AMS in the rigidity range from 2.1 to 21 GV for ^{4}He and from 1.9 to 15 GV for ^{3}He, each with half of the current statistics [11]. There have been measurements of deuteron and helium isotope fluxes and their ratios as functions of the kinetic energy per nucleon with large (∼40%) errors [12–16]. There are no previous measurements of D/^{4}He flux ratio as a function of rigidity.

In this Letter, precision measurements of D, ^{3}He, and ^{4}He fluxes and their ratios are presented with rigidity from 1.9 to 21 GV, based on 21 million D, 28 million ^{3}He, and 197 million ^{4}He nuclei collected by AMS from May 2011 to May 2021. The fluxes have been measured in 30 time periods of four Bartels rotations each (108 days).

The total time-averaged flux error at 10 GV is 3.0% for D, 2.3% for ^{3}He, and 1.6% for ^{4}He.

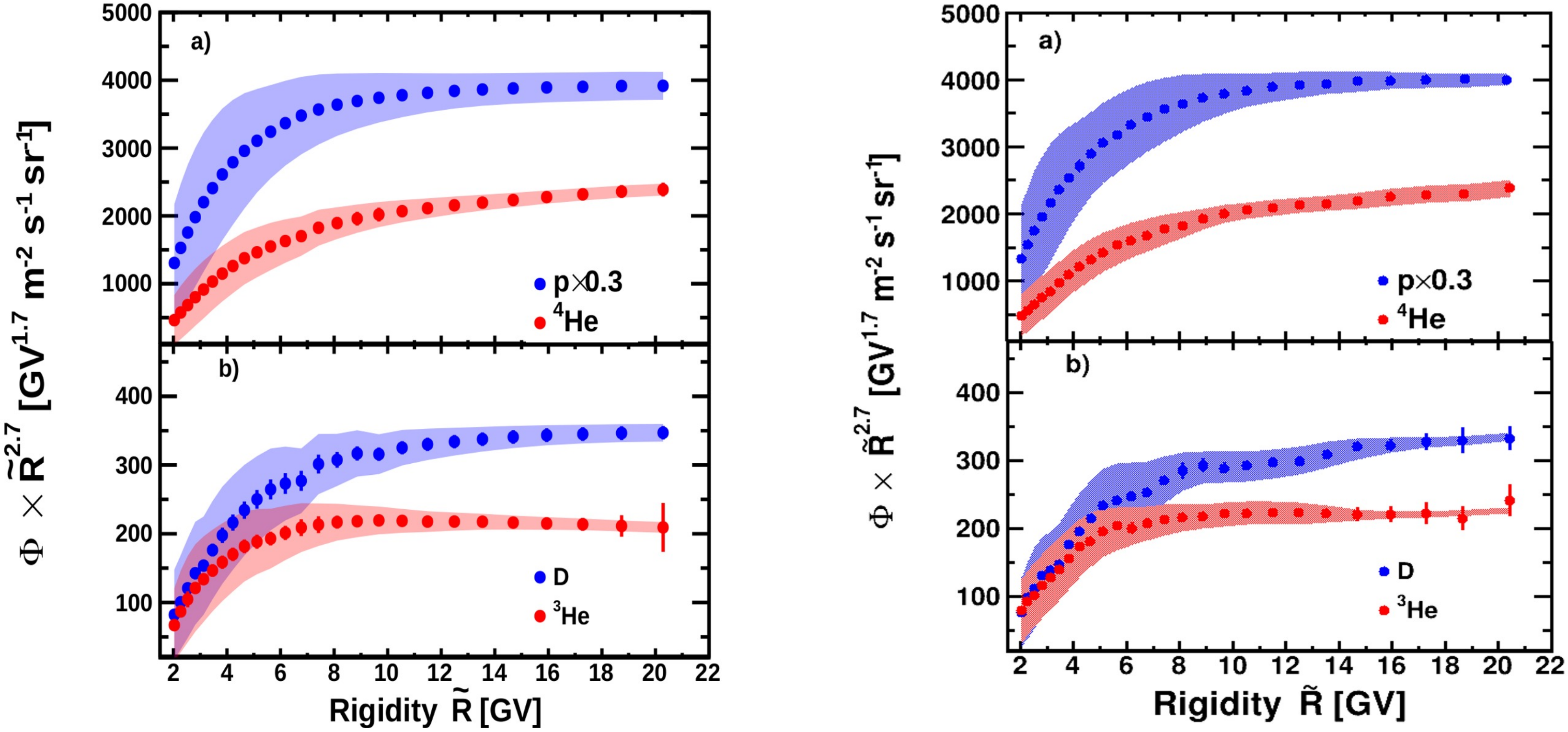

CIEMAT

TIPFA

FIG. 1. a) AMS time-averaged ^{4}He (red) and proton (blue) fluxes multiplied by $\tilde{R}^{2.7}$ as functions of rigidity with total errors. For display purposes, proton flux is scaled by a factor 0.3. b) AMS time-averaged ^{3}He (red) and D (blue) fluxes, multiplied by $\tilde{R}^{2.7}$ as functions of rigidity with total errors. The shaded regions show the range of the time variation of the fluxes.

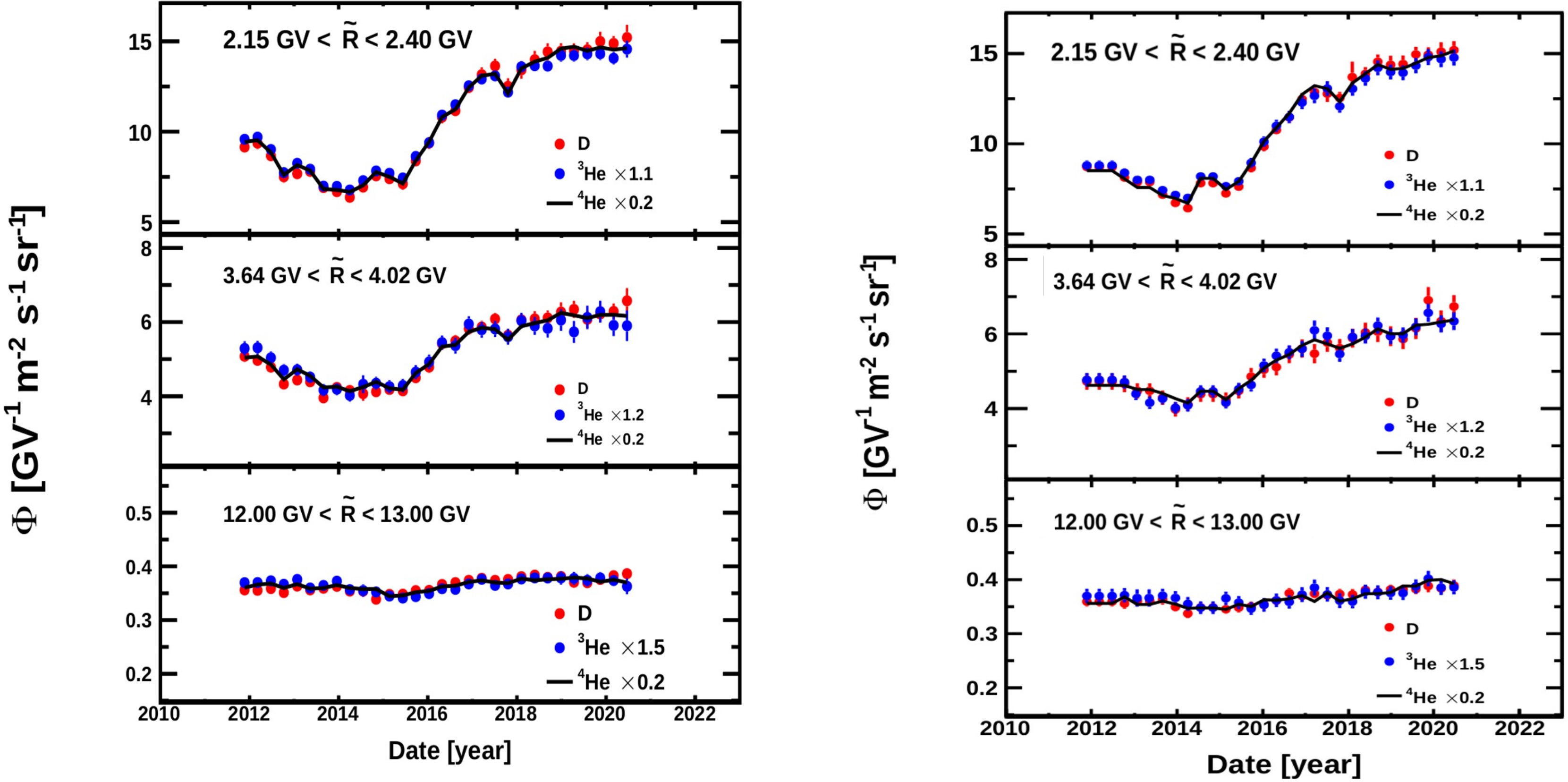

CIEMAT

TIPFA

FIG. 2. The AMS D (red points), ^{3}He (blue points), and ^{4}He (black curves) fluxes as functions of time for three rigidity bins. The ^{3}He and ^{4}He fluxes have been scaled to obtain the same time-averaged flux as D in each rigidity bin. The errors are the quadratic sum of the statistical and time-dependent systematic errors. In each rigidity bin the three fluxes show a nearly identical time behavior.

CIEMAT

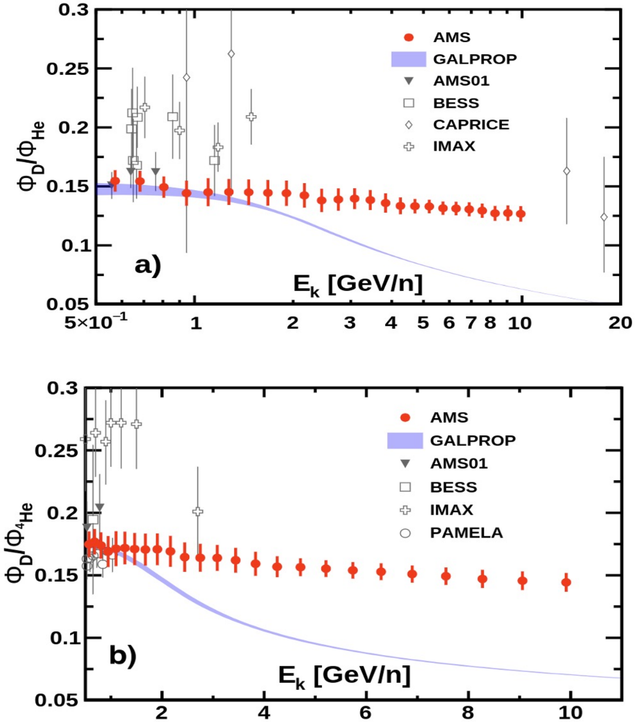

TIPFA

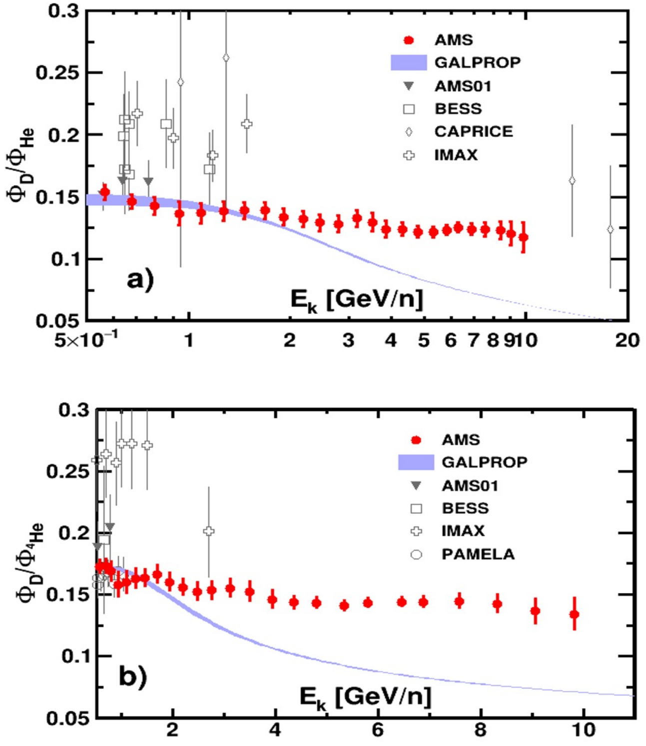

FIG. 3. The AMS a) D/(^{3}He +^{4}He),b) D/^{4}He, and ^{3}He/^{4}He flux ratios as functions of kinetic energy per nucleon with total error, together with previous measurements [12–16] and the cosmic ray latest propagation model GALPROP [35] predictions (shaded areas). The areas show the uncertainty of GALPROP prediction due to different solar modulation during the time period of the AMS observations.

CIEMAT

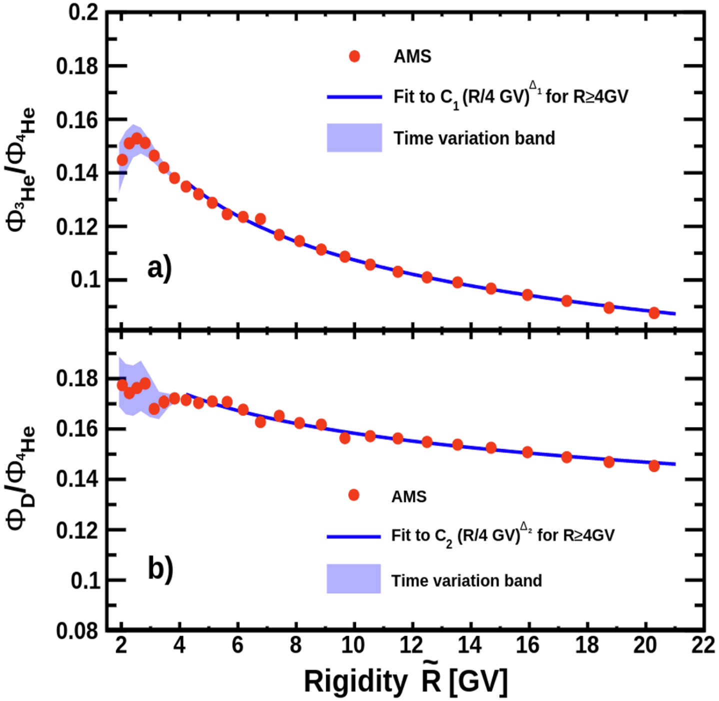

χ^2 / ndf	20/ 17
Δ_1	-0.288 ± 0.004
C_1	0.140 ± 0.002
χ^2 / ndf	11 / 17
Δ_2	-0.108 ± 0.005
C_2	0.175 ± 0.003

TIPFA

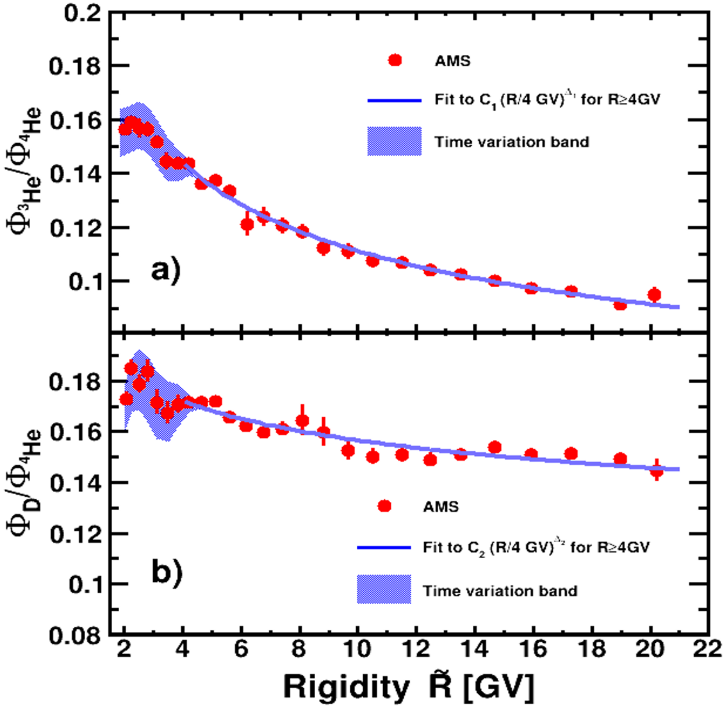

χ^2 / ndf	10 / 17
Δ_1	-0.284 ± 0.009
C_1	0.144 ± 0.002
χ^2 / ndf	22/ 17
Δ_2	-0.104 ± 0.008
C_2	0.174 ± 0.001

Comparison on D/^{4}He

Error bars TIFPA:

Stat. (+ uncorr. syst)	$\langle\sigma_S\rangle$/sqrt(N)	v
Fit systematic	$\langle\sigma_F\rangle$	v
Unfolding syst.	$\langle\sigma_U\rangle$	v
Acceptance error	$\langle\sigma_A\rangle$	x

Error bars CIEMAT:

Statistical	$\langle\sigma_S\rangle$/sqrt(N)	v
Unfolding	$\langle\sigma_u\rangle$	v
Corr	$\langle\sigma_c\rangle$	v
Acceptance	$\langle\sigma_A\rangle$	x

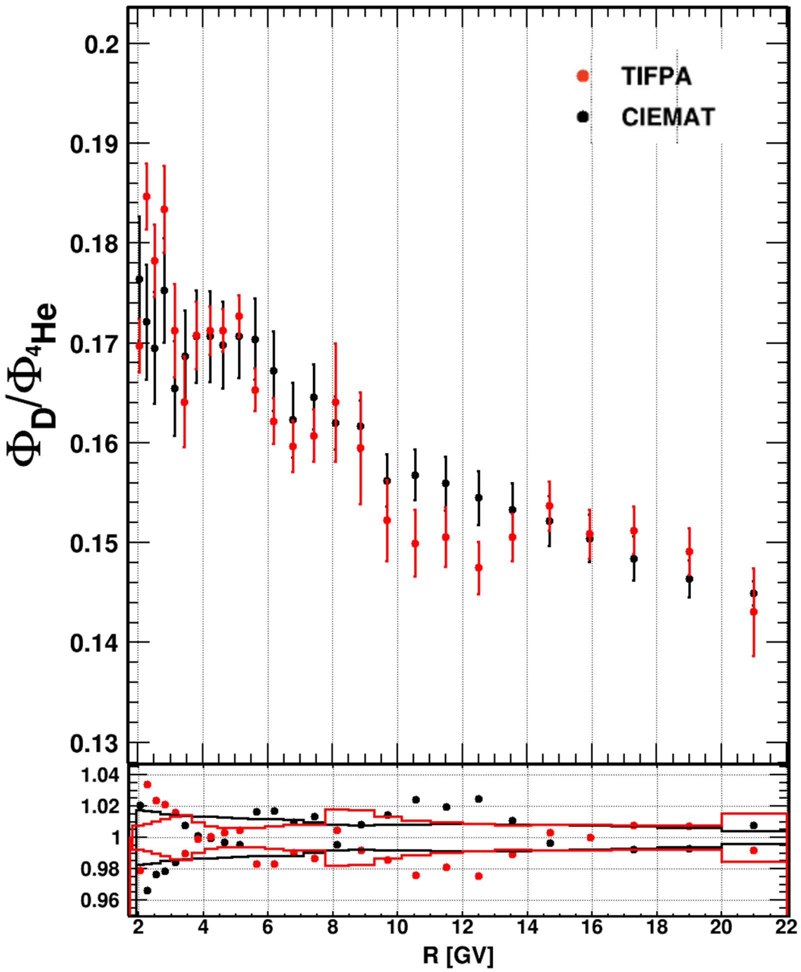

Isotopes flux ratios

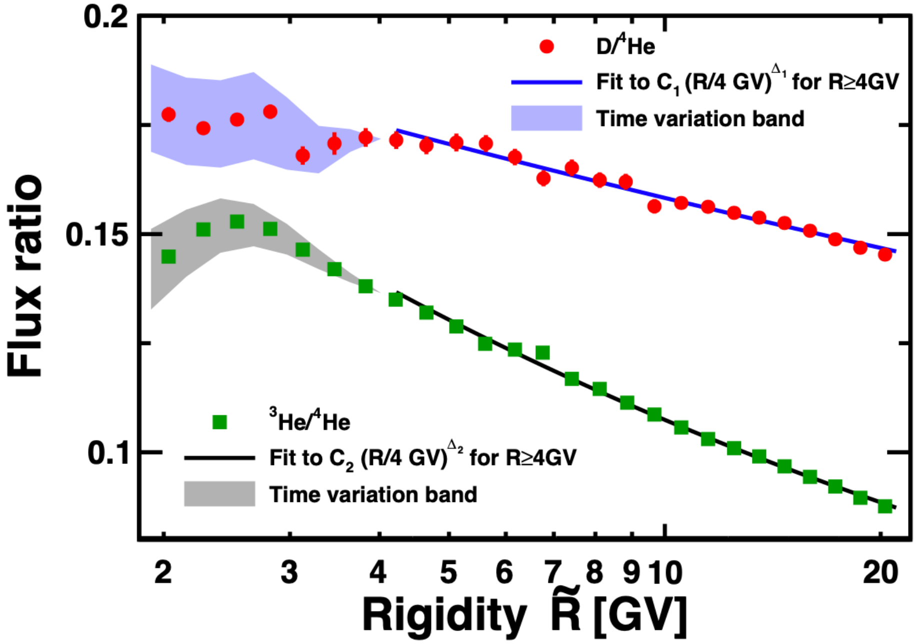

FIG. 4. AMS time-averaged D/^{4}He (red circles) and ^{3}He/^{4}He (green squares) flux ratios as functions of rigidity with statistical and uncorrelated systematic errors added in quadrature. Solid blue and black curves show power law fits $C\,(R/4\text{GV})^{\Delta}$ for R > 4 GV to the D/^{4}He and ^{3}He/^{4}He flux ratios respectively. Shaded areas show their time variation. For D/^{4}He flux ratio the fit yields: $\Delta_1 = -0.108 \pm 0.003$ and $C_1 = 0.175 \pm 0.004$ with $\chi^2/d.o.f.$ of 11/17. For ^{3}He/^{4}He flux ratio the fit yields: $\Delta_2 = -0.290 \pm 0.002$ and $C_2 = 0.140 \pm 0.003$ with $\chi^2/d.o.f.$ of 21/17.

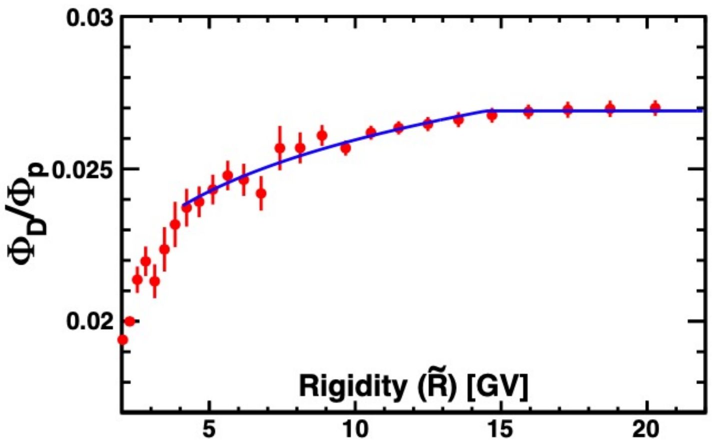

FIG. S7. The AMS D/p flux ratio as a function of rigidity with total errors. The blue curve shows the fit result of $C\,(R/R_0)^{\Delta}$ for 4GV < R < R$_0$; C for R ≥ R$_0$. The fit yields $C = 0.027 \pm 0.001$, $\Delta = 0.09 \pm 0.01$ and R$_0$ = 14 ± 1 with a $\chi^2/d.o.f.$ of 8.6/16. As seen, above R$_0 \simeq$ 14GV the D/p flux ratio is compatible with a constant.

Background from He fragmentation above L1

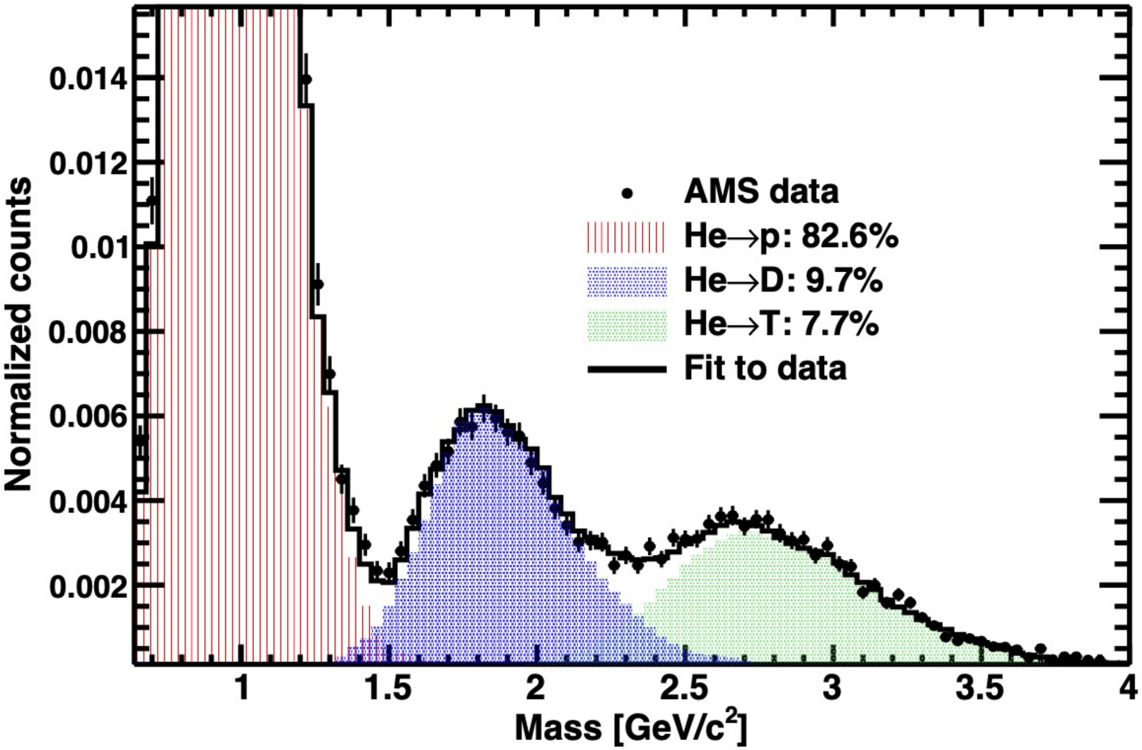

FIG. S2. Mass distribution of He events interacting between L1 and L2 with $0.6 < E_k < 0.75$ GeV/n for data (black points) and p, D and T templates (red, blue and green histograms) obtained from MC simulation. The black line shows the template fit to the data. The events were selected by requiring a measured charge Z=2 in tracker L1 and charge Z=1 in the inner tracker (L2-L8).

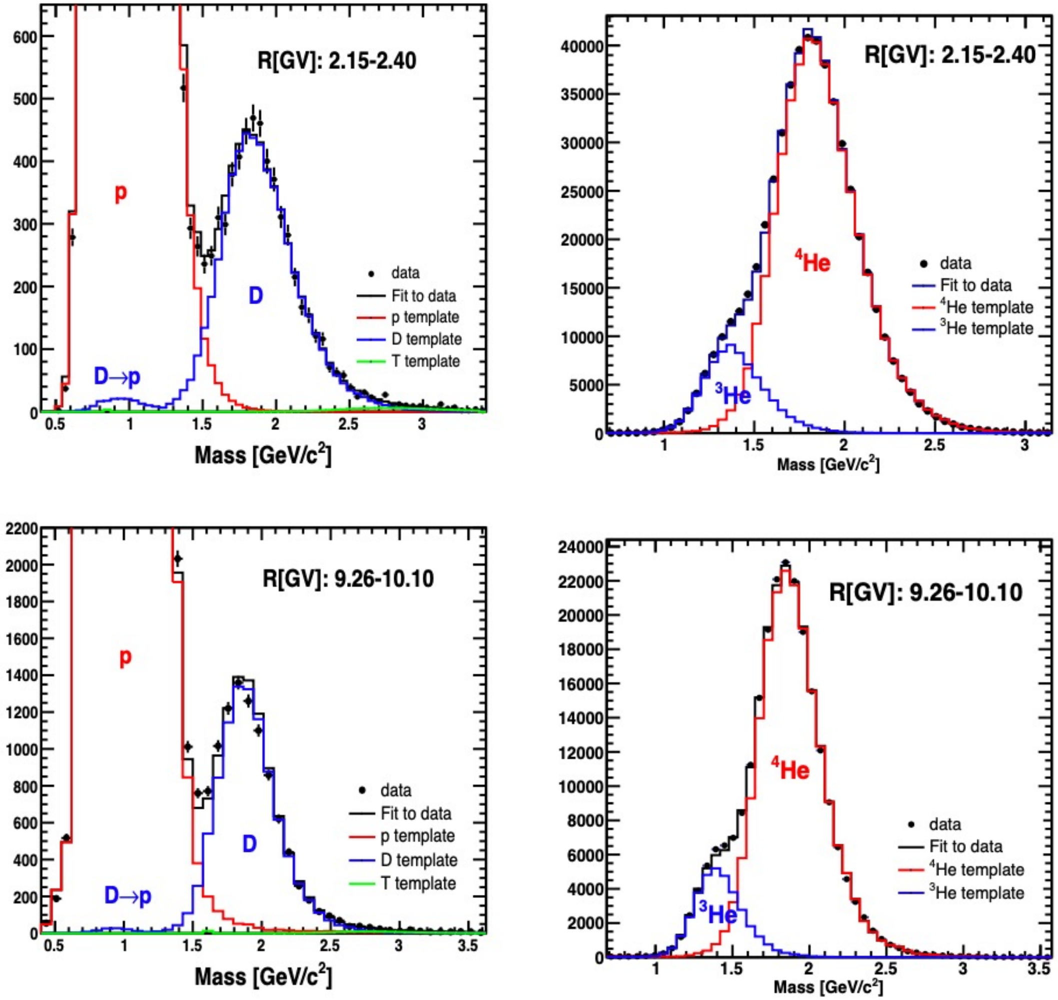

FIG. S3. Reconstructed mass distributions for Z=1 events (a and c) and for Z=2 events (b and d) for two velocity intervals corresponding to the two rigidity intervals for D of $2.15 < R[GV] < 2.40$ using β from TOF (top) and $9.26 < R[GV] < 10.10$ using β from RICH-Agl (bottom). The figures show also the template fit to the data and its contributions.

Modelling beta resolution

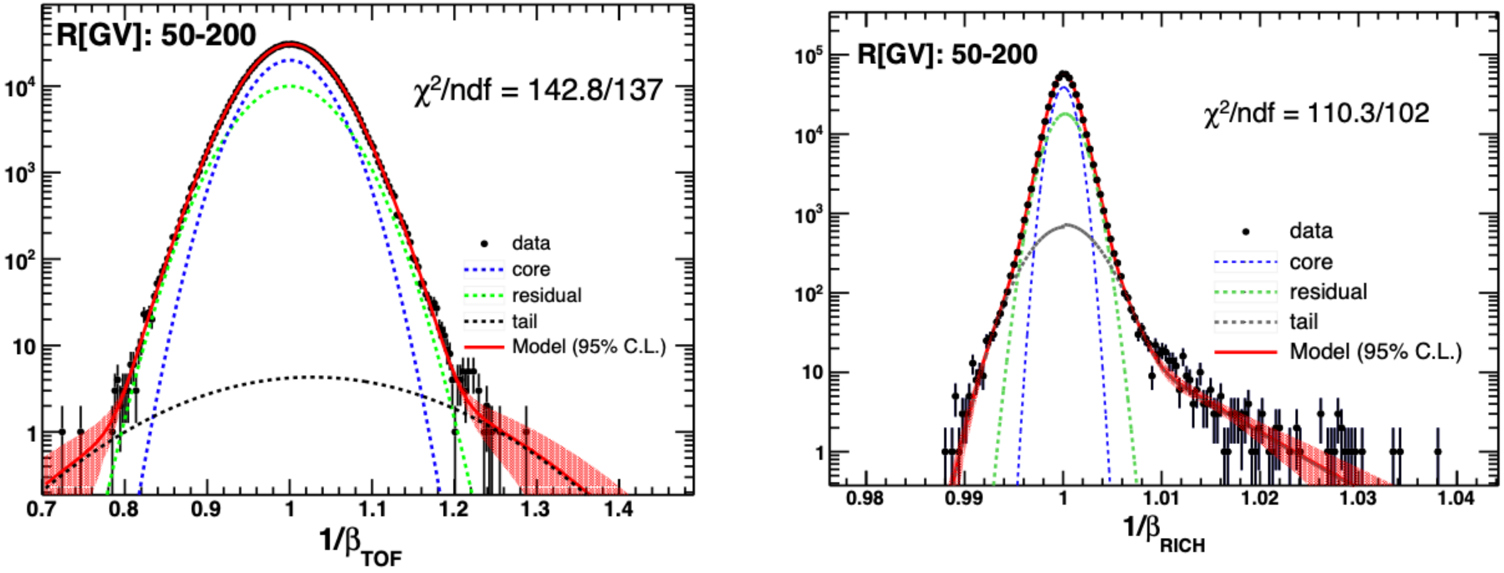

FIG. S4. Reconstructed inverse velocity ($1/\beta$) distributions at high rigidity ($50 < R[GV] < 200$) for Z=1 events obtained using TOF (a) and RICH-Agl (b). Such distributions are modeled (red continuous line) with the combination of a Gaussian core (blue dashed) and a second Gaussian residual distribution (green dashed), with the addition of a third Gaussian + power law tail distribution modeling the residual combinatory tail (black dashed).

Isotopes flux ratios

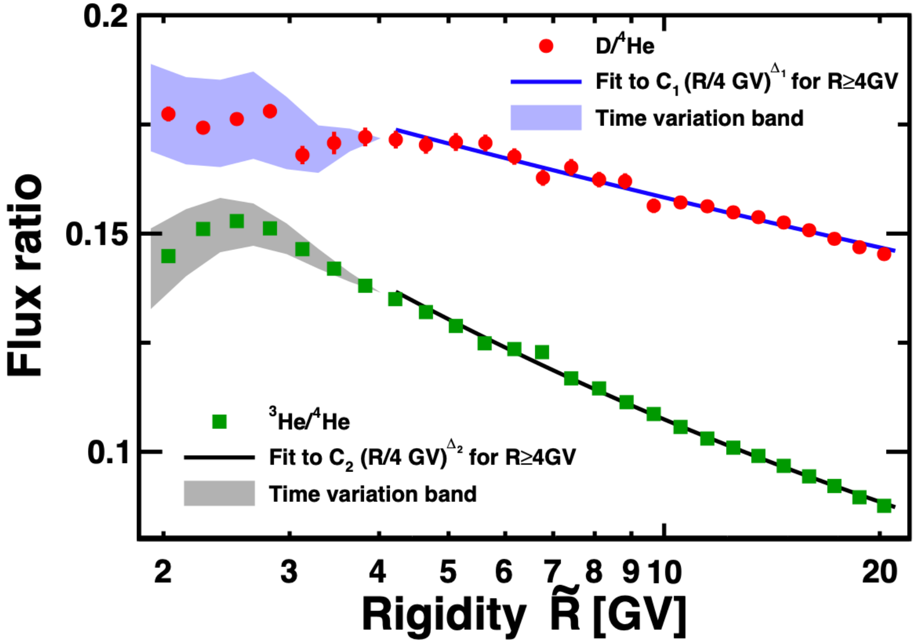

FIG. 4. AMS time-averaged $D/^4He$ (red circles) and $^3He/^4He$ (green squares) flux ratios as functions of rigidity with statistical and uncorrelated systematic errors added in quadrature. Solid blue and black curves show power law fits $C\,(R/4GV)^{\Delta}$ for R > 4 GV to the $D/^4He$ and $^3He/^4He$ flux ratios respectively. Shaded areas show their time variation. For $D/^4He$ flux ratio the fit yields: $\Delta_1 = -0.108 \pm 0.003$ and $C_1 = 0.175 \pm 0.004$ with $\chi^2/d.o.f.$ of 11/17. For $^3He/^4He$ flux ratio the fit yields: $\Delta_2 = -0.290 \pm 0.002$ and $C_2 = 0.140 \pm 0.003$ with $\chi^2/d.o.f.$ of 21/17.

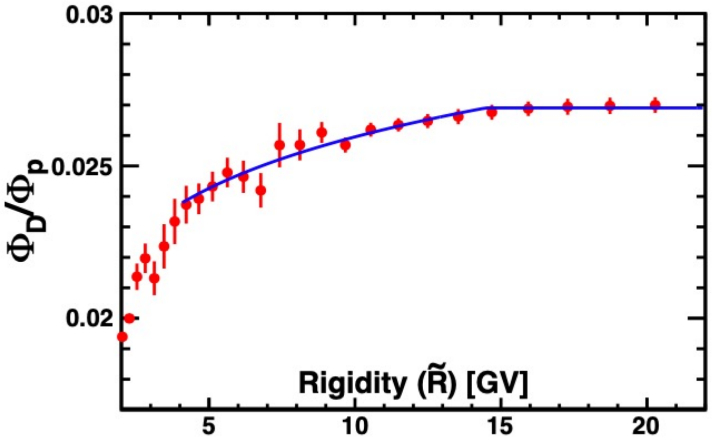

FIG. S7. The AMS D/p flux ratio as a function of rigidity with total errors. The blue curve shows the fit result of $C\,(R/R_0)^{\Delta}$ for 4GV < R < R_0; C for R ≥ R_0. The fit yields $C = 0.027 \pm 0.001$, $\Delta = 0.09 \pm 0.01$ and $R_0 = 14 \pm 1$ with a $\chi^2/d.o.f.$ of 8.6/16. As seen, above $R_0 \simeq$ 14GV the D/p flux ratio is compatible with a constant.

Low energy time dependence

$$\frac{\Phi^i_{(\mathrm{D},^3\mathrm{He})}/\Phi^i_{^4\mathrm{He}}}{\langle \Phi^i_{(\mathrm{D},^3\mathrm{He})}/\Phi^i_{^4\mathrm{He}}\rangle} - 1 = k^i_{(\mathrm{D},^3\mathrm{He})} \cdot \left(\frac{\Phi^i_{^4\mathrm{He}}}{\langle \Phi^i_{^4\mathrm{He}}\rangle} - 1\right)$$

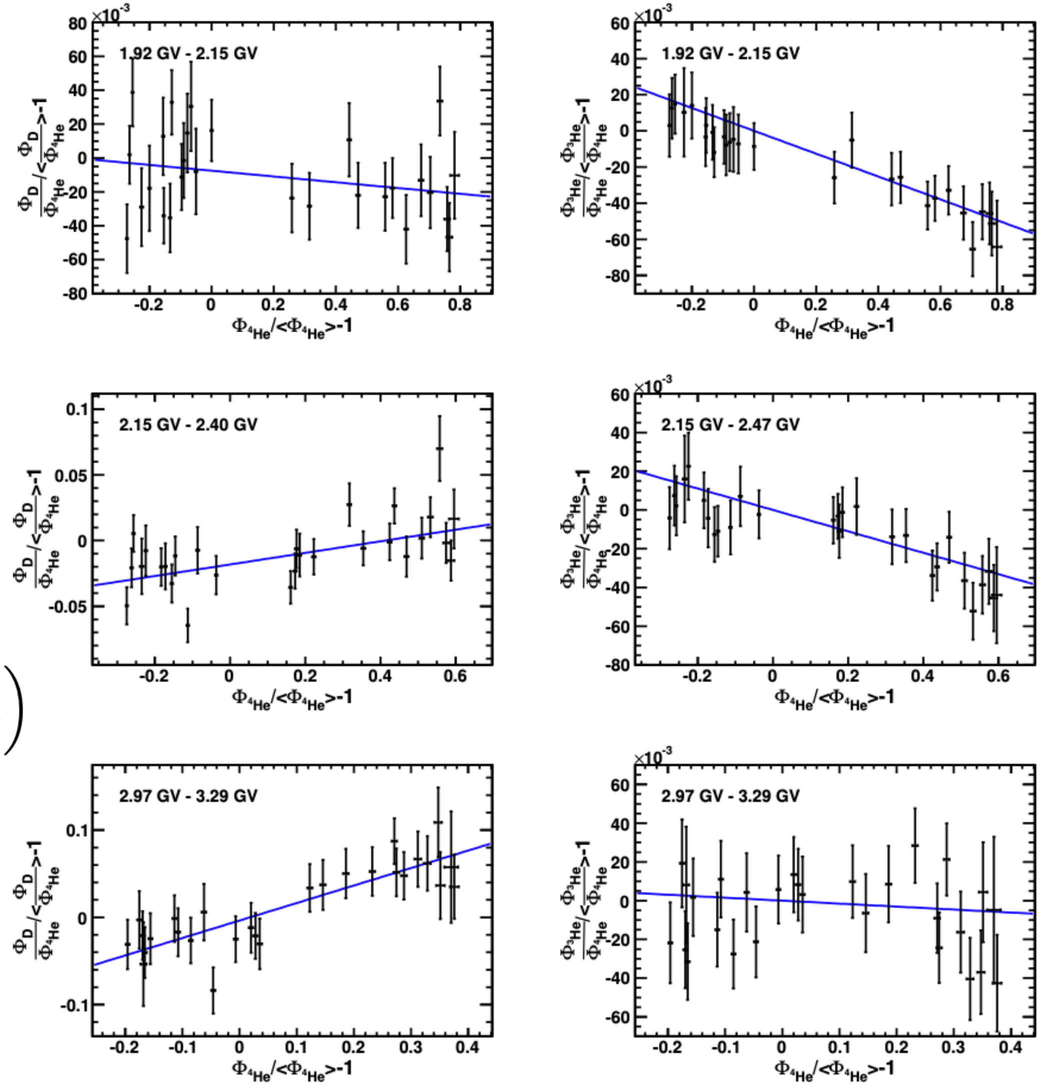

FIG. S5. The AMS D/^{4}He and ^{3}He/^{4}He flux ratios as function of ^{4}He flux for three characteristic rigidity bins. The blue lines show the fit with Eq. (3) result.

Low energy time dependence

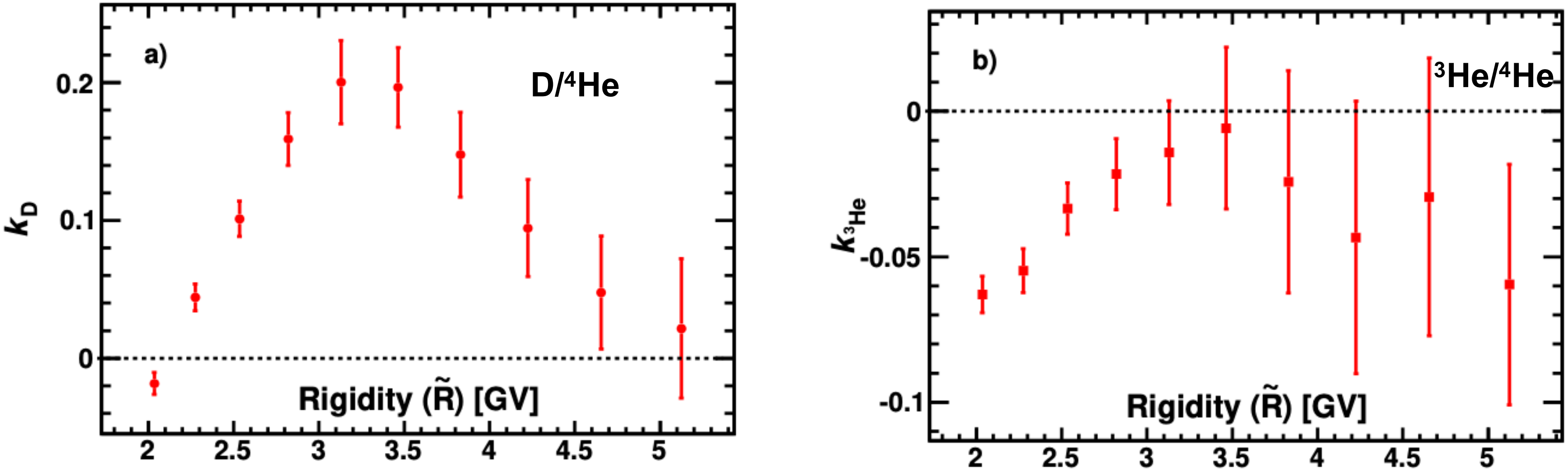

FIG. S6. Eq 3 k_i fitted values for a) D/^{4}He and b) ^{3}He/^{4}He flux ratios as function of rigidity.

$$\frac{\Phi^i_{(\mathrm{D},^3\mathrm{He})}/\Phi^i_{^4\mathrm{He}}}{\langle\Phi^i_{(\mathrm{D},^3\mathrm{He})}/\Phi^i_{^4\mathrm{He}}\rangle} - 1 = k^i_{(\mathrm{D},^3\mathrm{He})} \cdot \left(\frac{\Phi^i_{^4\mathrm{He}}}{\langle\Phi^i_{^4\mathrm{He}}\rangle} - 1\right)$$

Summary

- **AMS-02 measured the ^{3}He and D fluxes using 10 years of data in the rigidity range from 2GV to 20 GV.**

- **Below ~4GV:** solar modulation induces a time evolution of the the measured fluxes larger than the systematics of the measurement.

- **Above ~4GV:** D/4He and 3He/4He flux ratios are time independent. Their rigidity dependence is well described by a single power law $\propto R^{\Delta}$ with

  $\Delta_1 = -0.108 \pm 0.003$ D/^{4}He

  $\Delta_2 = -0.290 \pm 0.002$ ^{3}He/^{4}He

  showing that cosmic rays D and ^{3}He have different rigidity dependence.

  The significance of $\Delta_1 > \Delta_2$ exceeds 10 σ.

  This shows that contrary to expectations, cosmic deuterons have a sizeable primary component

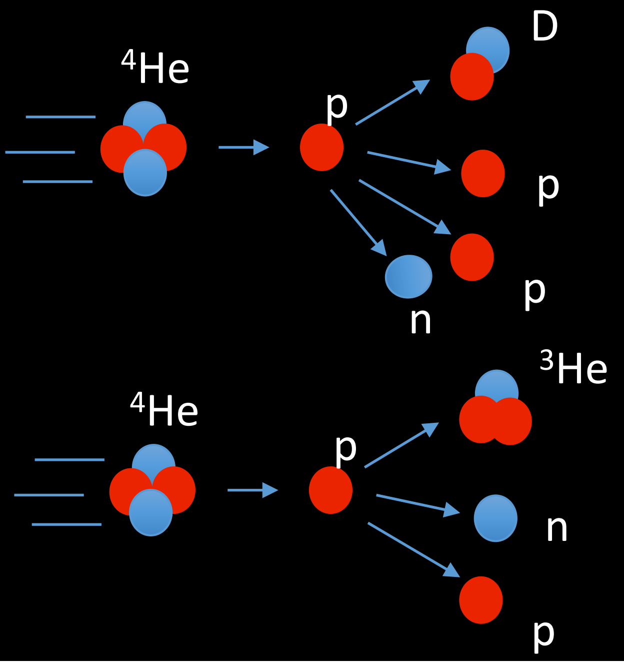

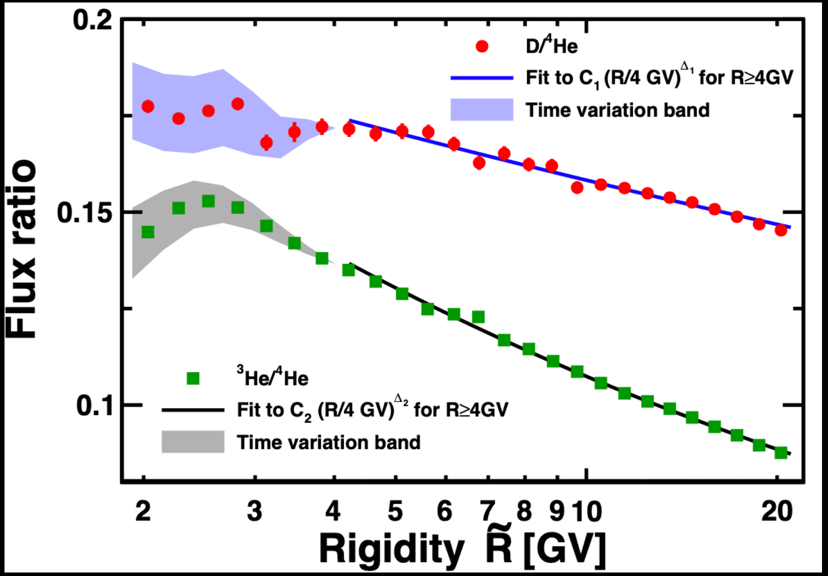

Thanks for your attention